Lab on a Chip

PAPER

View Article Online
View Journal | View Issue

Cite this: *Lab Chip*, 2025, **25**, 6256

Evaluating anti-sickling therapies for sickle cell disease: a microfluidic assay for red blood cell-mediated microvascular occlusion under hypoxia

Zoe Sekyonda, †[a] Yuxuan Du, †[b] Solomon Oshabaheebwa, [a] Payam Fadaei, [b] Yusang B. Ley,[a] Calvin Abonga, [c] Michael A. Suster, [c] Pedram Mohseni [ac] and Umut A. Gurkan *[abd]

Sickle cell disease (SCD) is characterized by the polymerization of hemoglobin S (HbS) upon deoxygenation, leading to the formation of sickled red blood cells (RBCs) with reduced deformability. Under hypoxic conditions, the impaired RBC behavior significantly contributes to vaso-occlusive events, hemolysis, and end-organ damage. Consequently, RBC deformability serves as a pivotal hemorheological biomarker for evaluating disease severity and therapeutic response. The OcclusionChip, a microfluidic assay, measures RBCs deformability through microcapillary occlusion. However, its current hypoxic assay relies on a complex nitrogen gas setup, rendering it bulky, expensive, and unsuitable for point-of-care diagnostic use. Here, we optimized a chemically induced hypoxia assay using sodium metabisulfite (SMB) within the OcclusionChip platform and validated the hypoxia occlusion index (HOI) as a robust measure of RBC deformability in SCD. Optimal hypoxia conditions were established, replicating nitrogen-induced hypoxia without affecting RBC membrane integrity, reactive oxygen species (ROS) levels, or phosphatidylserine (PS) exposure. Under these conditions, RBCs from individuals with heterozygous (HbAS), HbSC, and HbSS genotypes showed significantly higher HOI compared to healthy controls (HbAA), correlating strongly with clinical biomarkers in SCD. Additionally, the HOI assay effectively assessed the efficacy of therapeutic agents, including hemoglobin-oxygen affinity modifiers (GBT021601, GBT440) and protein kinase R (PKR) activators (PKR-3, FT4202), which significantly reduced OI in SCD RBCs. Notably, combination therapies showed enhanced effectiveness, highlighting the assay's potential for optimizing treatment regimens. This study establishes the chemically induced hypoxia OcclusionChip assay as a reliable and clinically useful tool for evaluating RBC deformability in SCD, with significant potential to improve personalized treatment strategies and thus patient outcomes.

Received 12th March 2025,
Accepted 23rd September 2025

DOI: 10.1039/d5lc00264h

rsc.li/loc

Introduction

Sickle cell disease (SCD) is a hereditary blood disorder resulting from a single-point mutation in the beta-globin gene, which leads to the production of abnormal hemoglobin S (HbS).[1] Under low oxygen conditions, HbS molecules polymerize and cause red blood cells (RBCs) to adopt rigid abnormal morphologies, including sickle, holly, and granular-shaped forms.[2] The most prevalent SCD genotypes are homozygous beta-S (HbSS) and heterozygous beta-S/beta-C (HbSC).[1,3,4] Sickling of RBCs significantly impairs their deformability, resulting in altered rheological properties and aggregates, which can lead to vaso-occlusive crises, hemolysis, and chronic hemolytic anemia which are the primary clinical manifestations of the disease.[1] Additionally, the reduced deformability of RBCs in SCD patients facilitates their entrapment in the microvasculature, causing tissue ischemia, pain, and organ damage.[3,5] RBC deformability evaluation and quantification hold great potential for determining the severity of the disease and the effectiveness of the therapeutic interventions.

Ektacytometry and microsphiltration are conventional techniques for assessing RBC deformability.[6–8] Although they provide valuable insights, these methods often fail to detect HbS-carrying RBCs with low HbS levels.[9,10] Ektacytometry

[a] *Department of Biomedical Engineering, Case Western Reserve University, Cleveland, OH, USA*
[b] *Department of Mechanical and Aerospace Engineering, Case Western Reserve University, Cleveland, OH, USA. E-mail: umut@case.edu; Tel: +1 (216) 368 6447*
[c] *Department of Electrical, Computer, and Systems Engineering, Case Western Reserve University, Cleveland, OH, USA*
[d] *Case Comprehensive Cancer Center, Case Western Reserve University, Cleveland, OH, USA*
† Equal contributions.

measures RBC population deformability using parameters such as the elongation index under controlled shear or osmotic gradients.[11] In contrast, recent advancements have introduced microfluidic devices like the OcclusionChip, which mimic the architecture of the capillary bed by allowing RBCs to flow through narrow microchannels that closely resemble *in vivo* microvasculature.[12,13] Notably, the OcclusionChip performs single-cell measurements and can detect individual RBCs with abnormal deformability that are missed by ektacytometry, highlighting the complementary strengths of these methods.[9] However, the current OcclusionChip hypoxia assay relies on nitrogen-induced hypoxia, which is complex, bulky, and expensive, limiting its practicality for point-of-care (POC) applications.[12,14,15] Hypoxia, characterized by reduced oxygen tension, plays a pivotal role in the pathophysiology of SCD by promoting the polymerization of HbS, leading to RBC sickling and subsequent vaso-occlusion. To accurately simulate hypoxic stress *in vitro*, this study utilizes chemically induced hypoxia using sodium metabisulphite (SMB). We have developed a novel hypoxia assay for the OcclusionChip that simplifies hypoxia induction while maintaining physiological relevance.

Advancements in understanding SCD pathophysiology have led to the development of novel therapeutics, including oxygen modifiers such as voxelotor (GBT440) and GBT021601 and protein kinase R (PKR) activators, which aim to enhance RBC deformability, reduce hemolysis, and prevent vaso-occlusive events.[16] GBT440, a HbS polymerization inhibitor, initially showed clinical benefit by allosterically increasing hemoglobin oxygen (Hb-O_2) affinity, thereby inhibiting polymer formation. However, it was voluntarily withdrawn from the market, reflecting the challenges in achieving long-term efficacy and clinical adoption for first-generation therapies.[17,18] This underscores the continued need for advanced *in vitro* platforms capable of rigorously evaluating both emerging and continued agents under physiologically relevant conditions. GBT021601 a second-generation HbS polymerization inhibitor with enhanced potency, shares a similar mechanism of action with GBT440.[19] In parallel, etavopivat (FT-4202) and PKR-3 are PKR activators that target RBC glycolytic regulation to improve RBCs deformability and mitigate hemolytic damages.[20,21]

In this work, we have optimized chemically induced hypoxia conditions using SMB in the OcclusionChip assay and validated the hypoxia occlusion index (HOI) as a robust measure for assessing RBC deformability in healthy (HbAA), heterozygous (HbAS) individuals and SCD patients with HbSS and HbSC genotypes. Furthermore, we have investigated the utility of the HOI in evaluating the effectiveness of various therapeutic agents, including both single treatments and combination therapies, in reducing RBC occlusion. We have found optimal conditions for chemically inducing hypoxia that effectively mimic nitrogen-induced environments without compromising RBC membrane integrity, reactive oxygen species (ROS) levels, or phosphatidylserine (PS) exposure which are critical determinants of RBC deformability and function. Under these optimized conditions, we demonstrated that RBCs from subjects with SCD exhibited elevated HOI levels that significantly correlate with hemolytic clinical biomarkers. Moreover, HOI effectively assessed the efficacy of various therapeutic agents in reducing RBC occlusion, highlighting its potential as a promising tool for monitoring treatment outcomes and guiding the development of targeted therapies. Overall, this study demonstrates HOI's utility as a reliable biomarker for evaluating disease severity in SCD.

Methods

Reagents

Sodium metabisulfite (SMB; $Na_2S_2O_5$, #161519) was purchased from Sigma-Aldrich (St. Louis, MO), 5-(and-6)-chloromethyl-2′,7′-dichloro-dihydro-fluorescein diacetate acetyl ester (CM-H_2DCF-DA, #C6827) from Fisher Scientific (Hampton, NH), Alexa Fluor® 647 Anti-Hemoglobin subunit alpha antibody (EPR3608 # 1 AB215919) from Abcam (Waltham, MA), PE Annexin V (AB_2869071, #560930) from BD Pharmingen™ (Franklin Lakes, NJ), and APC anti-human (glycophorin A) (CD235a, #349113) from BioLegend (San Diego, CA). Unless indicated otherwise, reagents were reconstituted and diluted in phosphate-buffered saline (PBS).

Blood sample collection and pilot clinical study

De-identified whole blood samples were collected from healthy individuals (HbAA) as controls and from patients with SCD (HbSS, HbSC) at University Hospitals Cleveland Medical Center (UHCMC) in Cleveland, Ohio. Blood was collected in ethylenediaminetetraacetic acid (EDTA) tubes. The study received ethical approval from the UHCMC Institutional Review Board and was conducted in accordance with the Declaration of Helsinki. Immediately following collection, blood samples were stored at 4 °C and processed within 10 hours. The HbSS, HbSC, HbAS genotype of the samples was confirmed using high-performance liquid chromatography with a Bio-Rad Variant II Instrument (Bio-Rad, Montreal, QC, Canada). Comprehensive clinical data, including white blood cell (WBC) count, platelet count, absolute neutrophil count (ANC), absolute reticulocyte count (ARC), RBC count, total hemoglobin (Hb), lactate dehydrogenase (LDH), mean corpuscular volume (MCV), creatinine (CRT), and serum ferritin levels for HbSS and HbSC samples, were obtained from the clinic at UHCMC on dates contemporaneous with blood samples collection. Details are in Table S1.

Preparation of RBC treatments with anti-sickling agents

Whole blood samples were centrifuged at 500*g* for 5 minutes at room temperature. Following centrifugation, the plasma layer and buffy coat were carefully removed and

discarded. Packed RBCs were then washed twice with PBS containing 5 mM glucose (PBS-G) and resuspended to a 20% hematocrit (v/v) in PBS-G supplemented with 0.6% (v/v) dimethyl sulfoxide (DMSO) to serve as the vehicle control. Control samples for each experiment included RBCs treated with vehicle DMSO without any drug. For RBCs treated with PKR-3 (HbSS + PKR-3) or etavopivat (HbSS + FT-4202), packed RBCs at 20% hematocrit in PBS-G were incubated for 6 hours at 37 °C with 200 μM PKR-3 (MedChemExpress, PKR-IN-2, Cat No. HY-19702) or FT-4202 (MedChemExpress, FT-4202, Cat No. HY-139573) dissolved in DMSO. The incubation was performed on a VWR Incubating Orbital Shaker 3500 (VWR International, Radnor, PA) set at 300 rpm. For RBCs treated with voxelotor (HbSS + GBT-440) or osivelotor (HbSS + GBT021601), HbSS RBCs at 20% hematocrit were mixed with 67 mg mL^{-1} of voxelotor (Selleckchem, GBT440, Cat No. S8540) or osivelotor (MedChemExpress, GBT021601, Cat No. HY-148788) in 100% DMSO to achieve a final concentration of 600 μM. These samples were then incubated at 37 °C for 6 hours on the VWR Incubating Orbital Shaker at 300 rpm. To prepare RBCs treated with both GBT021601 and FT-4202 (HbSS + GBT021601 + FT-4202), packed RBCs at 20% hematocrit in PBS-G were incubated for 6 hours at 37 °C with 200 μM PKR-3 in DMSO and 67 mg mL^{-1} of osivelotor in 100% DMSO to achieve a final concentration of 600 μM. The incubation was carried out on the VWR Incubating Orbital Shaker at 300 rpm. All treatments were conducted under identical conditions to ensure consistency across experimental groups.

OcclusionChip fabrication and functionalization

The OcclusionChip (Fig. 1A and B) was fabricated using established soft lithography techniques.[12,13] As previously described, the device consists of nine micropillar arrays that create microcapillaries narrowing from 20 μm to 4 μm along the flow direction, complemented by two 60 μm-wide side passageways. This microfluidic architecture mimics the non-uniform, dynamic capillary beds observed *in vivo*.[13] Following fabrication, the chip was serially rinsed with 100% ethanol and 1X PBS to ensure thorough cleaning. It was then incubated overnight at 4 °C with a 2% bovine serum albumin (BSA) solution to block non-specific binding sites. This functionalization step minimizes non-specific adhesion of RBCs, thereby enhancing the specificity and reliability of RBC occlusion assays performed within the chip.

Occlusion assay procedures

Normoxic conditions. RBCs at 20% hematocrit were introduced into the chip and perfused for 15 minutes using non-permeable tubing connected to a constant inlet pressure

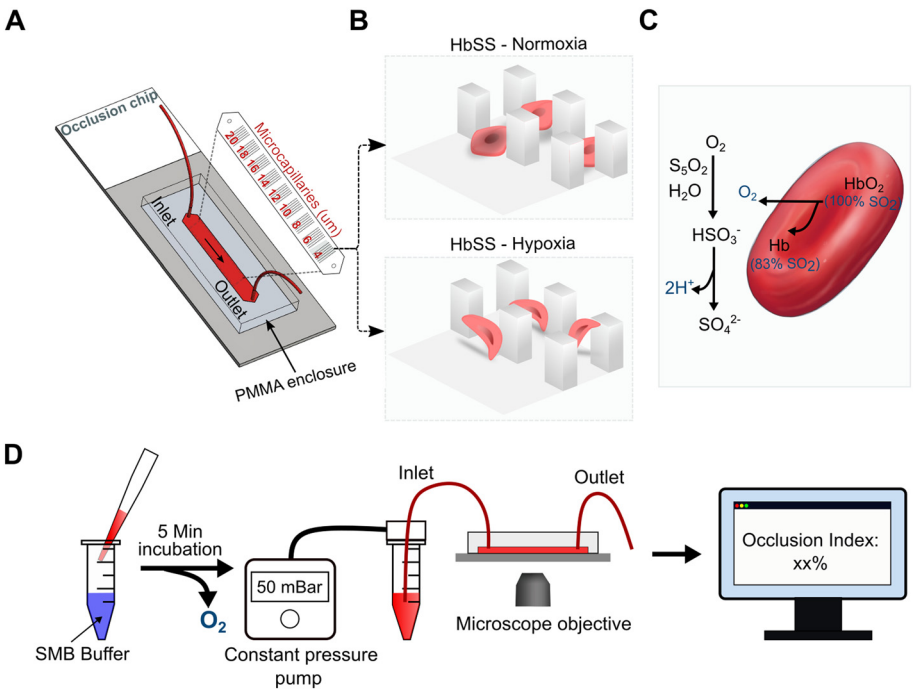

Fig. 1 Schematic illustration of occlusion devices used to assess hypoxia-induced red RBC sickling. (A) Assembly of the OcclusionChip, featuring microcapillaries with diameters decreasing from 20 μm to 4 μm along the flow direction to retain deformed RBCs. (B) 4 μm micropillar array demonstrating that non-deformed HbSS RBCs traverse the micropillars under normoxic conditions, whereas deformed HbSS RBCs occlude the micropillars under induced hypoxia. (C) Sequential chemical reaction of SMB in PBS-G buffer eliminates extracellular oxygen (O_2), creating a hypoxic environment necessary for RBC sickling. (D) Experimental setup for chemically inducing hypoxia-mediated sickling: RBC suspension was combined with SMB buffer and incubated for 5 minutes to achieve depletion in partial pressure of oxygen of $pO_2 \sim 44$ mmHg. Deoxygenated RBCs were perfused into the OcclusionChip using a constant inlet pressure pump set at 50 mbar for 10 minutes. Images of the OcclusionChip mounted on an inverted microscope were captured, and the percentage of OI was quantified using cell counting software.

pump set at 50 mbar (Flow-EZ™, Fluigent, Lowell, MA). Following perfusion, the microfluidic channel was visualized using an Olympus IX83 inverted motorized microscope. The occlusion index (OI), which measures the percentage of occlusion within the microcapillary network under normoxia, was calculated for regions encompassing micropillar arrays ranging from 4 μm to 10 μm in inter-pillar distance (Fig. 1A). For each sample, a single representative image was analyzed. Occluded RBCs within these micropillar arrays were manually counted using Adobe Photoshop CC, and the occlusion percentage was quantified using a previously published algorithm. Details of the equation used to calculate OI are shown in Notes S1.

Hypoxic conditions. To simulate a hypoxic environment, the OcclusionChip was configured with a micro-gas exchanger consisting of permeable tubing nested within non-permeable tubing. This assembly was filled with a gas mixture of 5% CO_2 and 95% N_2, achieving an oxygen saturation (SO_2) level of 83% at the microchannel inlet.[12,14] Under these standard gas-induced hypoxic conditions, RBCs were introduced into the OcclusionChip using the same hematocrit and perfusion settings as the normoxic assays.

Chemically induced hypoxia

Sodium metabisulphite (SMB) was employed to deoxygenate RBC samples. SMB hydrolyzes in PBS-G to form bisulfite ions (HSO_3^-), which react with the extracellular environment to reduce oxygen levels, thereby lowering the partial pressure of oxygen (pO_2) (Fig. 1C). Initially, RBCs at 20% hematocrit were mixed with varying concentrations of SMB (5%, 2%, 1.5%, and 1%) using a vortex mixer (Scientific Industries, Bohemia, NY) and incubated for different durations to achieve gradual pO_2 reduction. Following optimization, subsequent experiments utilized a fixed SMB concentration of 1.5% and an incubation time of 5 minutes. Oxygen levels were verified using a fiber optic oxygen sensor (NeoFox-GT; Ocean Optics, Orlando, FL). Details of the ratio of both dissolved oxygen and RBC-bound oxygen to SMB molecules are shown in Table S2.

Control RBCs and treated HbSS RBCs (HbSS + PKR-3, HbSS + FT4202, HbSS + GBT-440, and HbSS + GBT021601) with 1.5% SMB were then perfused into the OcclusionChip following the same protocol as the normoxic assays. After perfusion, the microchannel was imaged, and the HOI was quantified as described above (Fig. 1D). Details of the equation used to calculate HOI are shown in Notes S1. We analyzed RBCs occlusion under normoxic, gas-induced hypoxic, and chemically induced hypoxic conditions.

Measurement of RBC oxidative stress

Oxidative stress in RBCs was assessed using the fluorescent probe CM-H2DCF-DA at 100 μM. RBCs at 20% hematocrit were incubated with CM-H2DCF-DA in PBS-G for 30 minutes at 37 °C in the dark to facilitate intracellular uptake and de-esterification of the probe. After incubation, RBCs were washed twice with PBS-G to remove excess dye. Fluorescence intensity, indicative of intracellular ROS levels, was measured using a BD LSRFortessa flow cytometer (Franklin Lakes, NJ). Median fluorescence intensity (MFI) was quantified as a proxy for oxidative stress within the RBCs. Negative control samples consisted of RBCs incubated without CM-H2DCF-DA. Positive controls included RBCs incubated with CM-H2DCF-DA and a mixture of hypoxanthine (HO; 2 mM) and xanthine oxidase (XO; 0.1 U mL^{-1}) to generate extracellular superoxide anion (SOA) and hydrogen peroxide. Additionally, positive controls were treated with phenazine methosulphate (PMS) at 0.01 mM to generate intracellular superoxide anion, as previously reported by Hannemann *et al.*[22] For test samples (RBCs + SMB), RBCs were incubated with CM-H2DCF-DA followed by treatment with 1.5% SMB. All measurements were performed in triplicate to ensure reliability. Details are described in Notes S2.

Measurement of RBC membrane integrity

The membrane integrity of RBCs was evaluated using the fluorescent dye Alexa Fluor 647. RBCs at a hematocrit of 0.01% were incubated with Alexa Fluor 647 (10 nM) in PBS for 15 minutes at room temperature in the dark to allow binding to compromised membranes. Following incubation, cells were washed twice with PBS-G to remove excess dye. Membrane integrity was analyzed using a BD LSRFortessa flow cytometer (Franklin Lakes, NJ), with fluorescence detected in the FL4 channel. Negative controls consisted of RBCs incubated with PBS-G alone, while positive controls included RBCs treated with *tert*-butyl hydroperoxide (*t*BHP) to induce membrane permeabilization. Test samples (RBCs + SMB) included RBCs treated with 1.5% SMB. MFI in the FL4 channel was quantified as an indicator of membrane integrity. All measurements were performed in triplicate to ensure reliability. Details are described in Notes S3.

Measurement of phosphatidylserine exposure

Phosphatidylserine (PS) exposure on RBCs was quantified using BD Pharmingen™ PE Annexin V and APC anti-human CD235a (glycophorin A).[23] RBCs at a hematocrit of 20% were stained with APC anti-CD235a and PE Annexin V in 1X PBS containing 10 mM calcium chloride for 30 minutes at room temperature. Stained and unstained RBCs were analyzed using a BD LSRFortessa flow cytometer. Negative control samples consisted of Tyrode's buffer with RBCs incubated without staining reagents. Positive control samples comprised Tyrode's buffer with 10 mM calcium chloride, RBCs, PE Annexin V, and APC anti-CD235a. Test RBC samples (negative + SMB) were only incubated with 1.5% SMB and Tyrode's buffer. Test RBC samples (positive + SMB) were incubated with 1.5% SMB, Tyrode's buffer with 10 mM calcium chloride, PE Annexin V, and 2.5 μL of APC anti-CD235a. Flow cytometry data

were analyzed using FlowJo software to calculate the percentage of PS-positive RBCs. All experiments were performed in triplicate to ensure reliability. Details are described in Notes S4.

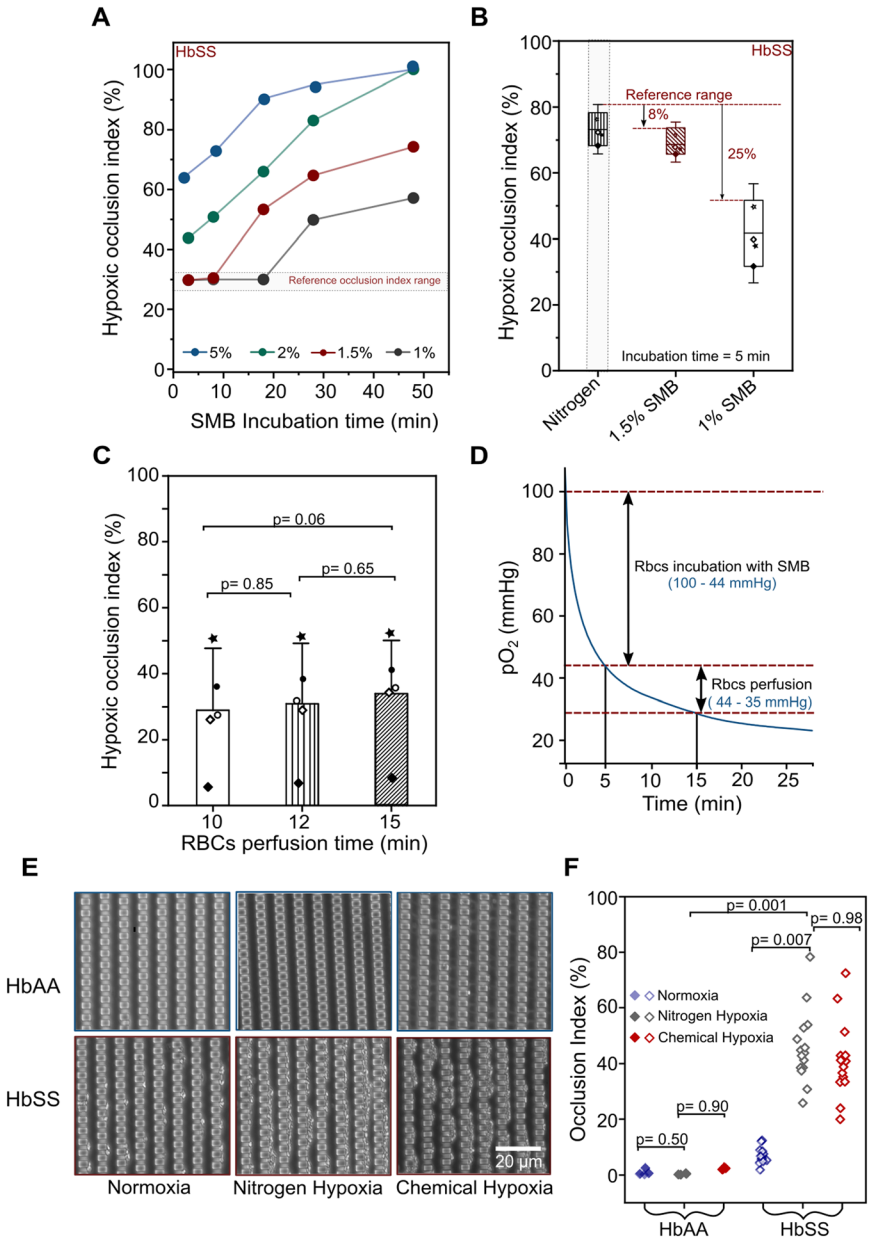

Fig. 2 Optimization of chemically induced hypoxia-mediated occlusion in the OcclusionChip using sodium metabisulphite (SMB) compared to nitrogen gas-induced hypoxia. (A) Reducing SMB concentration from 5% to 1% and incubation time from 50 to 5 minutes at 20% hematocrit achieved optimal HOI conditions comparable to nitrogen-induced hypoxia. (B) For HbSS RBCs, HOI at 1.5% SMB and 5-minute incubation was not significantly different from nitrogen-induced HOI (8% difference; p = 0.58, n = 4, Wilcoxon test). However, HOI at 1% SMB was significantly lower, showing a 25% difference compared to nitrogen-induced HOI (p = 0.007, n = 4, Wilcoxon test). (C) For HbSS RBCs, at 1.5% SMS, HOI values showed no significant differences between 10, 12, and 15 minutes of RBC perfusion into the OcclusionChip ($p > 0.05$ for all comparisons, n = 5, Friedman-test). (D) pO_2 kinetics under chemically induced hypoxia: incubation of HbAA RBCs with 1.5% SMB for 5 min lowered pO_2 from 100 mmHg to ~44 mmHg; perfusion into the OcclusionChip further decreased pO_2 from 44 mmHg to ~35 mmHg by 10 min, where it stabilized between 32–23 mmHg through 20 min (n = 5). The blue line represents measured pO_2 data for a representative HbAA sample. (E) Representative microcapillary occlusion images from HbSS and HbAA subjects under normoxia, nitrogen-induced hypoxia, and chemically induced hypoxia. (F) Comparison of microcapillary HOI showed no significant differences for HbAA RBCs between normoxic and hypoxic conditions (p = 0.50, n = 6, Wilcoxon test). HbSS RBCs exhibited significantly increased HOI under both nitrogen-induced and chemically induced hypoxia compared to normoxia (p = 0.007, n = 15, paired t-test). There were no significant differences between HOI values under nitrogen-induced hypoxia and chemically induced hypoxia for both HbAA (p = 0.90, n = 6, paired t-tests) and HbSS RBCs (p = 0.98; n = 15, paired t-tests). HbSS RBCs had significantly higher HOI compared to HbAA RBCs under chemically induced hypoxia (p = 0.001; HbAA n = 5, HbSS n = 15; Mann–Whitney test). n represents RBCs from different individuals. Error bars are presented as SD.

Statistical analysis

Statistical analysis was performed using Minitab® software (Release 2021, Version 20; Minitab). Sample responses for each patient were evaluated pairwise between treated and untreated groups using either a paired *t*-test or a one-Wilcoxon signed-rank test, as appropriate. For multiple comparisons involving non-parametric data, a Friedman test with Dunn's correction was applied, while one-way ANOVA with Tukey's *post hoc* analysis was used for normally distributed data with more than two groups. The Mann–Whitney U-test was used for non-parametric comparisons between two groups. Pearson's correlation analysis was used to assess correlations for only HbSC and HbSS patient samples. Samples with missing clinical laboratory test values were excluded from the correlation analysis. $P < 0.05$ was considered statistically significant. Data are reported as mean ± standard deviation (SD).

Ethical statement

All experiments were performed in accordance with the Guidelines of the United States Food and Drug Administration (US FDA) and Declaration of Helsinki and approved by the ethics committee at the University Hospitals Cleveland Medical Center (UHCMC IRB# 05-14-07C). Informed consents were obtained from human participants of this study.

Results

Optimization of chemically induced hypoxia assay in the OcclusionChip

To optimize the chemically induced hypoxia assay in the OcclusionChip, we systematically evaluated various concentrations of SMB (1% to 5%) and incubation times (5, 10, and 15 minutes) in both HbAA and HbSS RBCs. Increasing SMB concentrations from 1% to 5% and extending incubation times correspondingly elevated the HOI in HbSS samples (Fig. 2A). Notably, a concentration of 1.5% SMB with a 5-minute incubation yielded HOI values comparable to those achieved with nitrogen gas-induced hypoxia (Fig. 2B), while a 1% concentration resulted in significantly lower HOI compared to the reference ($p < 0.05$). Consequently, 1.5% SMB and a 5-minute incubation were identified as the optimal conditions for chemically inducing hypoxia in the occlusion assay. Further assessment of RBC perfusion times into the OcclusionChip revealed that HOI values at 10, 12, and 15 minutes were not significantly different ($p > 0.05$), indicating consistent assay performance across these durations (Fig. 2C). During the 5-minute incubation of HbAA RBCs with 1.5% SMB, the partial pressure of oxygen (pO_2) decreased from 100 mmHg to 44 mmHg and further reduced from 44 mmHg to ~35 mmHg by 15 minutes RBCs perfusion (Fig. 2D and S1). Comparative analysis between HbAA and HbSS samples under normoxic, nitrogen-induced hypoxic, and chemically induced hypoxic conditions (1.5% SMB for 15 min assay) demonstrated that HbAA RBCs exhibited HOI values under normoxia (1.16 ± 0.67%) that were not significantly different from those under both hypoxia conditions (1.34 ± 0.1%; $p > 0.87$; Fig. 2E and F). In contrast, HbSS RBCs showed significantly lower occlusion index (OI) under normoxia (8.19 ± 1.43%) compared to both hypoxic conditions ($p < 0.05$; 52.67 ± 6.02%) nitrogen-induced hypoxia and (48 ± 3.46%) chemically induced hypoxia (Fig. 2E and F). These results indicate that 1.5% SMB with a 5-minute incubation and a 10-minute perfusion time effectively mimics standard nitrogen gas-induced hypoxia, providing a reliable model for assessing RBC occlusion under hypoxic stress.

Hypoxia induction maintains ROS levels, membrane integrity, and PS exposure in RBC

To evaluate the effects of chemically induced hypoxia on RBCs, we assessed intracellular ROS levels, membrane

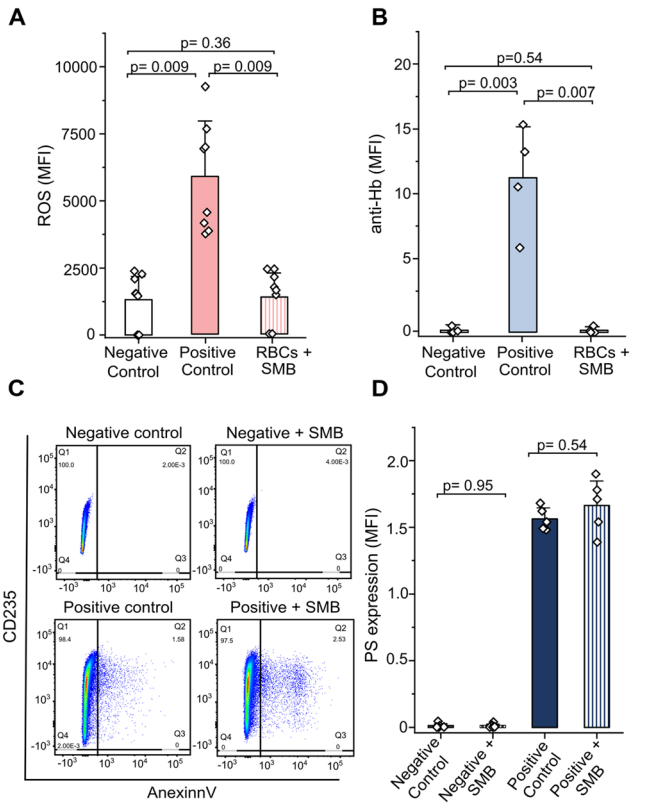

Fig. 3 Chemical hypoxia induction does not increase intracellular ROS, disrupt membrane integrity, or enhance PS exposure in HbAA RBCs. (A) Intracellular ROS levels in HbAA RBCs treated SMB were comparable to negative controls and significantly different from positive controls (p = 0.002, n = 8). (B) Anti-hemoglobin immunoglobulin labeling showed no difference in Hb-negative RBCs between those treated with SMB and negative control groups, whereas Hb-positive RBCs were significantly different (p = 0.007, n = 4). (C) Representative images display PS exposure in negative and positive control RBCs with and without SMB treatment. (D) PS exposure in treated RBCs with SMB was similar to both negative and positive controls (p = 0.006, n = 5). Statistics were performed using the non-parametric Wilcoxon test and Friedman multiple comparison test. n represents RBCs from different individuals. Error bars are presented as mean ± SD.

integrity, and PS exposure following treatment with SMB on HbAA. Elevated ROS and PS exposure levels have been reported as surrogate markers of hemolysis, membrane damage, and impaired RBC deformability.[24,25] Treatment with SMB did not significantly alter intracellular ROS levels in HbAA RBCs compared to negative controls (p = 0.36) (Fig. 3A). However, SMB-treated RBCs showed significantly different ROS levels than positive controls (p = 0.009), indicating that SMB does not induce excessive ROS production under the tested optimal conditions. Membrane integrity, assessed *via* anti-hemoglobin immunoglobulin labeling, revealed no significant difference in HbAA-negative RBCs and RBCs with SMB (p = 0.54) (Fig. 3B). In contrast, HbAA-positive RBCs exhibited a considerable difference when treated with SMB compared to controls (p = 0.007), suggesting selective effects on membrane integrity in Hb-positive cells. Additionally, PS exposure in SMB-treated RBCs was comparable to both negative (p = 0.95) and positive controls (p = 0.54) (Fig. 3C and D), indicating that SMB treatment did not enhance PS exposure in HbAA RBCs. These findings demonstrate that hypoxic occlusion assay effectively mimics physiological hypoxia without increasing intracellular ROS, disrupting membrane integrity, or enhancing PS exposure under optimal conditions. Consequently, SMB treatment maintains RBC viability and membrane integrity while accurately modeling hypoxic stress.

HOI assesses pathological impaired RBC deformability in hemoglobin S (HbS)-related abnormalities and correlations with clinical parameters

We investigated the clinical and pathophysiological relevance of the hypoxic OcclusionChip assay by evaluating RBCs from 15 adult subjects with HbAS, 5 with HbSC, 14 with HbSS, and 5 with HbAA. Under optimal conditions, the HOI significantly increased in HbS carriers, including HbAS

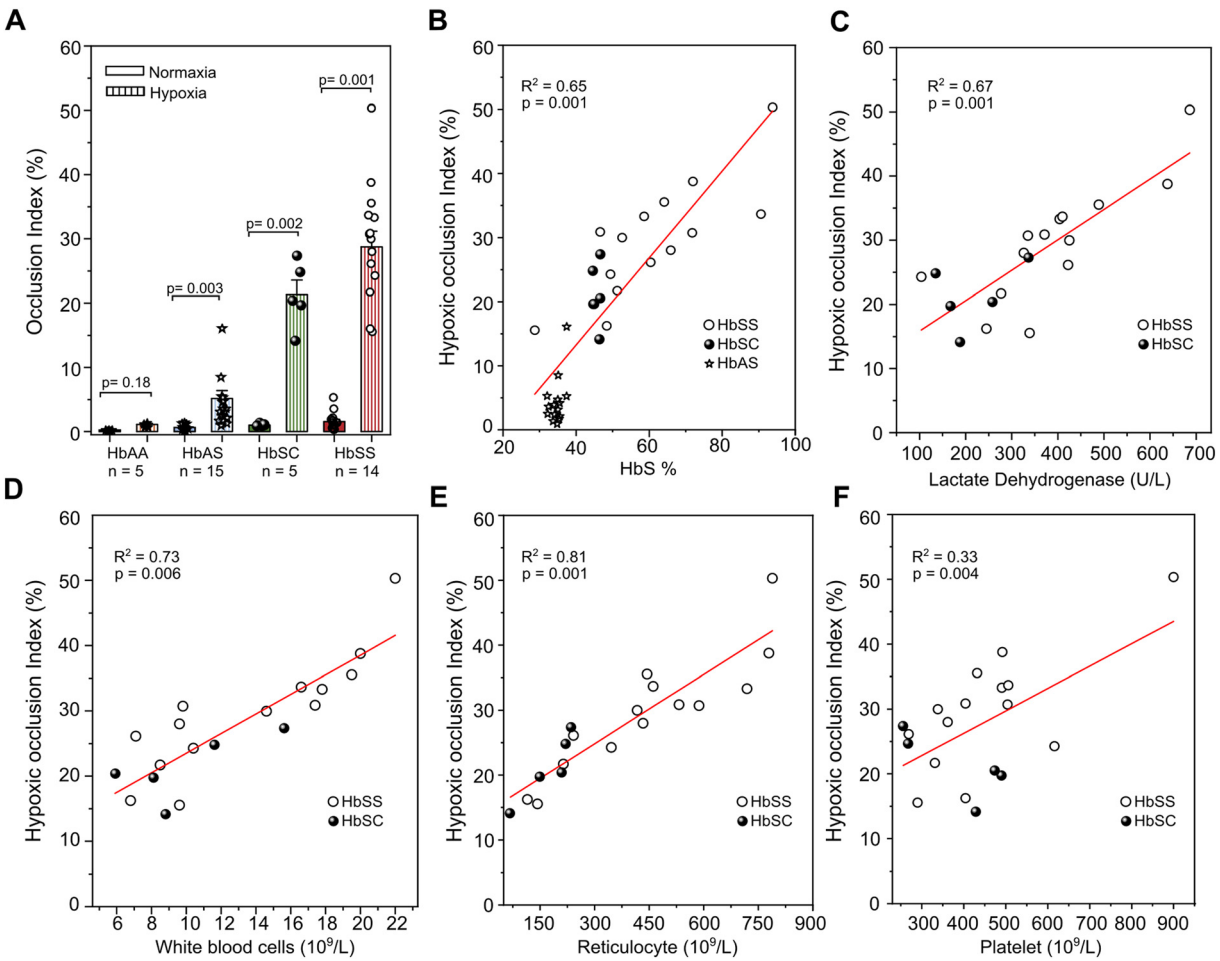

Fig. 4 HOI detects hemoglobin S (HbS)-related RBC abnormalities and correlates with clinical parameters in subjects with HbSS and HbSC. (A) HOI significantly increased in HbS carriers: (HbAS: n = 15, p = 0.003; HbSC: n = 5, p = 0.002; HbSS: n = 14, p = 0.001; paired t-test), whereas HbAA RBCs showed no significant response (n = 5, p = 0.18, paired t-test). (B) HOI positively correlated with HbS levels in HbS-carrying RBCs: HbSS (n = 14), HbAS (n = 15), and HbSC (n = 5) (R^2 = 0.65, p = 0.001). In subjects with HbSS (n = 14) and HbSC (n = 5), HOI was significantly associated with: (C) lactate dehydrogenase (LDH) levels (R^2 = 0.67, p = 0.001), (D) white blood cell (WBC) count (R^2 = 0.73, p = 0.006), (E) reticulocyte count (R^2 = 0.81, p = 0.001), and (F) platelet count (R^2 = 0.33, p = 0.004). Each symbol represents a different genotype. n represents RBCs from different individuals. Error bars are presented as mean ± SD.

(n = 15, p = 0.003), HbSC (n = 5, p = 0.002), and HbSS (n = 14, p = 0.001) RBCs. In contrast, HbAA RBCs showed no significant response (n = 5, p = 0.18) between normoxic and hypoxic conditions (Fig. 4A). Among HbS carriers, HbSS RBCs exhibited the highest HOI, followed by HbSC and HbAS, indicating a gradient of impaired RBC deformability corresponding to the severity of the genotype. Additionally, we assessed hemolytic biomarkers, including LDH, HbS level, white blood cells, reticulocytes, and platelets. HOI positively correlated with HbS levels in HbS-carrying RBCs (R^2 = 0.65, p = 0.001) (Fig. 4B). In subjects with HbSS (n = 14) and HbSC (n = 5), the HOI was significantly associated with LDH levels (R^2 = 0.67, p = 0.001), white blood cell (WBC) count (R^2 = 0.73, p = 0.006), reticulocyte count (R^2 = 0.81, p = 0.001), and platelet count (R^2 = 0.33, p = 0.004) (Fig. 4C–F). These results indicate that HOI detects HbS-related RBC abnormalities and correlates with key clinical biomarkers in individuals with HbSS and HbSC.

HOI effectively evaluated therapeutic interventions targeting hemoglobin S (HbS)-carrying RBCs in subjects with HbSS and HbSC genotypes

We further explored whether hypoxic OcclusionChip assays could measure the effectiveness of RBC-targeted treatments. We evaluated four therapeutic agents, GBT021601, GBT440,

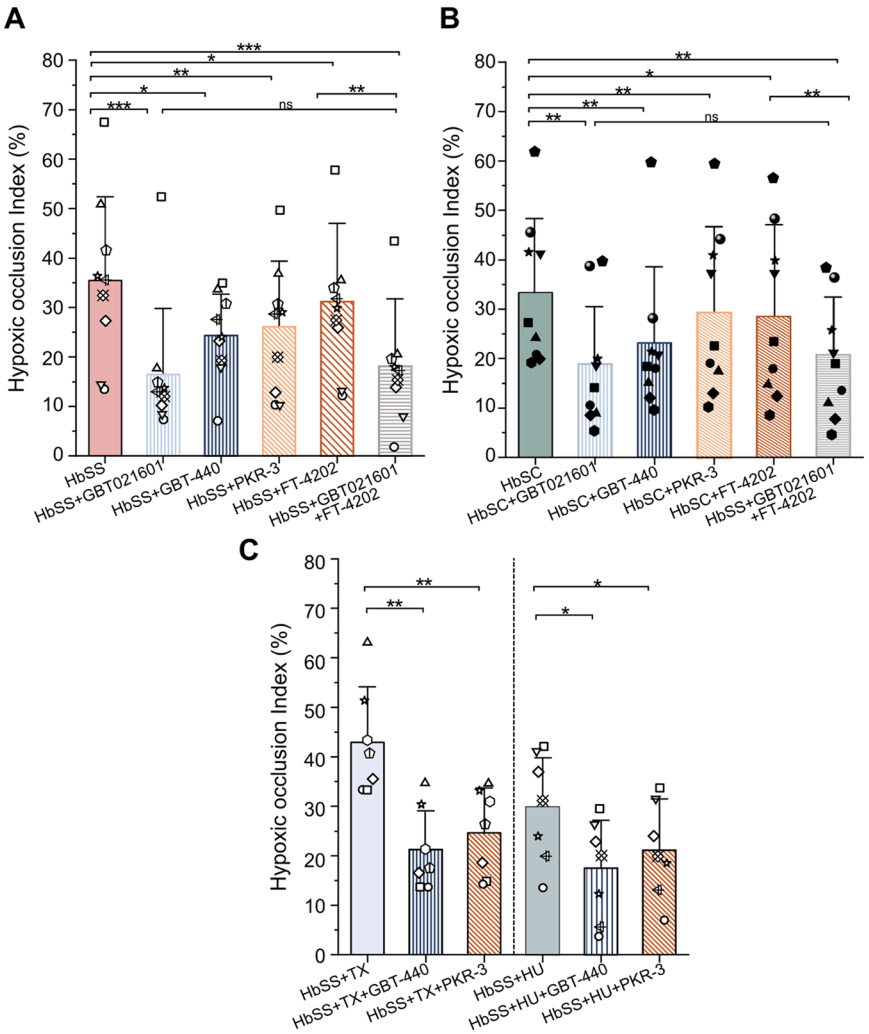

Fig. 5 HOI used as a tool for evaluating therapeutic interventions in hemoglobin S (HbS) – carrying RBCs. (A) HbSS RBCs (n = 9, each patient sample is represented by an empty symbol): Treatment with the oxygen modifiers GBT021601, GBT440, and the PKR activators PKR-3 and FT4202 each significantly reduced HOI compared to untreated cells. The GBT021601 + FT4202 combination further decreased HOI *versus* untreated RBCs and *versus* FT4202 alone but did not differ from GBT021601 alone. (B) HbSC RBCs (n = 9, each patient sample is represented by a filled symbol): GBT021601, GBT440, PKR-3, and FT4202 each lowered HOI relative to untreated controls. The GBT021601 + FT4202 combination further reduced HOI *versus* untreated RBCs and *versus* GBT021601 alone, with no significant difference from FT4202 alone. (C) HbSS RBCs from patients on transfusion therapy (TX) or hydroxyurea (HU) (n = 7; each patient sample is represented by an empty symbol): *ex vivo* addition of GBT440 or PKR-3 significantly lowered HOI compared to TX or HU-treated samples alone. For (A–C), statistics were performed using the paired test and the Wilcoxon test ***$p < 0.001$, **$p < 0.01$, *$p < 0.05$, ns not statistically significant. n represents RBCs from different individuals. Data are shown as mean ± SD.

PKR-3, and FT4202, and their combinations on RBCs from 19 subjects with SCD undergoing transfusion therapy (TX) or hydroxyurea treatment (HU), and 9 subjects with HbSC receiving supportive treatment. In HbSS RBCs, treatment with oxygen modifiers GBT021601 and GBT440, as well as PKR activators PKR-3 and FT4202, significantly reduced the HOI compared to untreated cells (GBT021601: 54.6% ± 15.02%, p = 0.0002; GBT440: 25.7% ± 28.69%, p = 0.012; PKR-3: 24.45% ± 14.15%, p = 0.001; FT4202: 12.89% ± 8.18%, p = 0.0109) (Fig. 5A). Additionally, the combination of GBT021601 and FT4202 resulted in a significantly lower HOI of 51.65% compared to untreated HbSS RBCs (p = 0.0001) and 44.40% ± 18.35% for FT4202 alone (p = 0.0039). However, it did not differ significantly from GBT021601 alone (p = 0.40). Similarly, in HbSC RBCs, treatment with GBT021601, GBT440, PKR-3, and FT4202 also significantly decreased the HOI compared to untreated controls (GBT021601: 46.38% ± 21.56%, p = 0.001; GBT440: 30.79% ± 23.31%, p = 0.008; PKR-3: 17.56% ± 16.56, p = 0.001; FT4202: 16.68% ± 20.59, p = 0.028) (Fig. 5B). The combination of GBT021601 and FT4202 further significantly reduced the HOI by 42.38% ± 19.43 compared to untreated HbSC RBCs (p = 0.0002) and 30.88% for FT4202 alone (p = 0.0014) but was not significantly different from GBT021601 alone (p = 0.089). Furthermore, in HbSS RBCs from patients undergoing *in vivo* TX or HU treatment, the addition of *in vitro* GBT440 or PKR-3 treatment significantly decreased the HOI compared to HbSS RBCs with TX or HU alone (TX + GBT440: 47.83% ± 24.20% p = 0.006; TX + PKR-3: 41.68 ± 21.18 p = 0.004; HU + GBT440: 31.78 ± 47.84 p = 0.039; HU + PKR-3: 20.61 ± 34.41, p = 0.04) (Fig. 5C). These results demonstrate that the hypoxia HOI can be utilized to assess the effectiveness of treatments. The HOI effectively detects reductions in RBC occlusion associated with HbS-related abnormalities when treated with therapeutics that share the same mechanism of action but belong to different generations.

Discussion

Hypoxia measurements in SCD are pivotal because low oxygen conditions fully trigger the severe characteristics of the SCD phenotype. Under hypoxia, hemoglobin S (HbS) polymerizes, causing RBCs to sickle and subsequently reduce their deformability.[3] This decreased flexibility impairs RBCs' ability to navigate blood vessels, leading to blockages and vaso-occlusive crises, which are primary contributors to pain and organ damage in SCD patients.[3,26] Therefore, accurate hypoxia measurement is essential for understanding and managing the pathological processes in SCD.

Here, we present a novel hypoxia assay optimized with the OcclusionChip microfluidic platform, which simulates microvascular flow conditions and quantifies RBC occlusion under hypoxic stress. By optimizing chemically induced hypoxia using SMB, we established a reliable method to achieve a pO_2 of 44–35 mmHg (~83% SO_2), closely mimicking mixed venous *in vivo* conditions without compromising RBC integrity. The optimal conditions identified were 1.5% SMB with a 5-minute incubation, effectively replicating nitrogen-induced hypoxia (~83% SO_2) without inducing excessive ROS production, membrane disruption, or PS exposure in RBCs. Importantly, PS exposure not only signals early apoptotic processes but also perturbs membrane mechanics by disrupting lipid asymmetry and altering bilayer curvature, leading to increased membrane rigidity and enhanced cytoskeletal crosslinking. This stiffening diminishes RBC deformability and raises the fraction of cells that occlude capillary-scale channels. In addition, exposed PS provides a procoagulant surface that promotes RBCs endothelial and RBCs platelet adhesion, further exacerbating microvascular occlusion in SCD.[22,27] Likewise, uncontrolled ROS generation can oxidize membrane proteins and lipids, promoting cytoskeletal crosslinking and RBCs stiffening.[22] By confirming negligible ROS increase and PS exposure under our optimized SMB protocol, we ensure that elevations in the hypoxia occlusion index derive from true hypoxic stiffening rather than oxidative or apoptotic artifacts of membrane phospholipid scrambling. Maintaining RBC viability under hypoxic conditions ensures that the HOI accurately reflects pathophysiological changes, addressing previous concerns that chemical agents might cause oxidative stress or membrane destabilization, thereby confounding deformability measurements.[28]

We demonstrated the capability of HOI as a robust measure for detecting impaired RBC deformability across different SCD genotypes (HbAS, HbSC, HbSS) while showing no significant changes in HbAA individuals. The gradient of HOI values, with HbSS exhibiting the highest occlusion, followed by HbSC and HbAS, aligns with the known clinical severity of these genotypes.[3,4] Importantly, the positive correlations between HOI and clinical biomarkers such as HbS levels, LDH, WBC count, reticulocyte count, and platelet count underscore the clinical relevance of HOI as an indicator of disease severity and hemolytic activity.[8,29] Mechanistically, elevated LDH reflects intravascular hemolysis and the resultant predominance of stiffer RBCs; reticulocytes, being larger and less deformable, further raise HOI; chronic inflammation increase WBC promotes oxidative modifications of membrane proteins and lipids; and activated platelets exacerbate microvascular occlusion through direct interactions with rigid RBCs.[30] These correlations are most pronounced in HbSS and attenuated in HbSC cohorts, mirroring the spectrum of hemolytic burden and inflammation.[31] Moreover, hydroxyurea (HU) therapy by increasing fetal hemoglobin levels dramatically reduces LDH, reticulocyte, WBC, and platelet counts, concomitantly lowering HOI and confirming its sensitivity as a surrogate marker for therapeutic response.[32] Together, our findings highlight HOI not only as a quantitative readout of RBC deformability but also as a potential surrogate for broader clinical manifestations of SCD in both diagnostic and prognostic contexts.[33–35]

The ability of the HOI to effectively evaluate the efficacy of various therapeutic agents is particularly noteworthy. Treatments with oxygen modifiers (GBT021601, GBT440) and protein kinase R (PKR) activators (PKR-3, FT4202) significantly reduced the HOI in both HbSS and HbSC RBCs, indicating improved RBC deformability and reduced vaso-occlusive potential.[20,36] The synergistic effects of combination therapies, such as GBT021601 with FT4202, further highlight the assay's capability to discern nuanced therapeutic interactions and optimize treatment regimens. These findings are consistent with the mechanisms of action of these agents, which aim to inhibit HbS polymerization and enhance RBC metabolic pathways to improve cell flexibility and lifespan.[19,37] Previous studies have demonstrated that HbS polymerization inhibitors and PKR activators can effectively reduce sickling and hemolysis, thereby alleviating clinical symptoms.[21,38] Our results extend these findings by providing a reliable *in vitro* method to quantitatively assess the therapeutic efficacy of such agents under hypoxic conditions that closely mimic the *in vivo* environment.

Consistent with John *et al.*, we also observed inter-patient variability in HOI reductions in patient samples undergoing transfusion and hydroxyurea therapy, reflecting differences in individual hematologic and physiochemical profiles.[39,40] Furthermore, RBCs treated with targeted agents GBT021601, GBT440, PKR-3, and FT4202 exhibited distinct response patterns across donors. Importantly, the HOI assay not only consistently detected improvements in RBC deformability for each pharmacologic intervention but also faithfully captured the magnitude of response unique to each donor. These findings underscore HOI's dual utility: it quantifies average treatment effects and sensitively resolves donor-specific variability across a spectrum of therapeutic modalities.

The recent market withdrawal of GBT440 emphasizes the importance of robust preclinical assessment tools for sickle cell therapeutics. While GBT440's mechanism of stabilizing the relaxed hemoglobin conformation offered initial promise, its discontinuation revealed gaps in our ability to predict long-term clinical viability.[18] Our HOI platform addresses this need by enabling high-throughput, standardized endpoint measurements of capillary occlusion under controlled hypoxia, allowing not only rapid re-evaluation of legacy compounds like voxelotor but also head-to-head comparison with novel agents such as GBT021601. By combining chemical hypoxia induction with single-cell resolution, the HOI assay can accelerate identification of candidates with durable efficacy, including both withdrawn first-generation inhibitors and next-generation molecules, and guide optimization of drug combinations to achieve sustained therapeutic benefit.

Traditional methods like ektacytometry, while valuable, often do not fully capture the dynamic and complex deformability of RBC.[9–11] Ektacytometry primarily measures deformability under static shear or osmotic stress.[7] In contrast, OcclusionChip's microfluidic design, combined with chemically induced hypoxia, offers a more physiologically relevant assessment and enables the subtle deformability changes that ektacytometry may miss, highlighting its sensitivity and specificity in evaluating RBC pathology in SCD.[9] This enhanced detection capability is crucial for identifying early or mild alterations in RBC deformability that could precede clinical complications, thereby enabling timely therapeutic interventions. Furthermore, we found the HOI to be highly repeatable between two independent users (Fig. S2), demonstrating the assay's reliability and ease of use. The measurement error associated with HOI was evaluated by repeated analyses of the same sample by both users. The observed inter-user coefficient of variation (COV) was 4.68%, while intra-user COVs were 9.2% for user 1 and 9.5% for user 2, indicating strong repeatability and reproducibility. These results suggest that measurement error is minimal and that HOI yields reliable and consistent values across users and repeated analyses. This high degree of consistency supports the OcclusionChip's potential for widespread adoption in both clinical and research applications.

Prior work by Du *et al.* employed a microfluidic platform with controlled gas environments to dynamically modulate oxygen tension and record real-time transit delays and flow retardation, underscoring the value of kinetic analyses of sickling behavior, which are recognized as critical determinants of vaso-occlusive risk.[41] Their work demonstrated that both deoxygenation kinetics and channel transit profiles serve as sensitive indicators of cell mechanical properties and polymerization propensity. Our chemically induced hypoxia approach achieves rapid, uniform deoxygenation without the need for external gas controllers, and the HOI provides a standardized, high-throughput endpoint measure of capillary-scale occlusion. By complementing Du *et al.*'s kinetic, real-time analyses with a simplified chemical induction and fraction-occluded[12] readout, our platform broadens the toolkit for assessing RBC deformability and vaso-occlusion risk under physiologically relevant hypoxic conditions.

Establishing the HOI as a reliable biomarker for RBC deformability has significant clinical implications. It offers a quantitative tool for assessing disease severity, monitoring progression, and evaluating therapeutic responses in SCD patients. It supports personalized medicine approaches where treatments can be tailored based on real-time deformability assessments. Additionally, the simplified chemically induced hypoxia assay enhances the feasibility of integrating the OcclusionChip into clinical workflows, facilitating its adoption in routine SCD management. The portability and scalability of this method address previous limitations associated with the complexity and cost of nitrogen-induced hypoxia systems.[42,43]

Future research could explore the longitudinal use of HOI in monitoring treatment efficacy and its predictive value for clinical outcomes such as vaso-occlusive crises and organ

damage. Expanding the range of therapeutic agents tested with this assay could provide deeper insights into their mechanisms and potential combinatory effects. Furthermore, investigating the relationship between RBC deformability and other cellular or molecular markers of SCD could enhance our understanding of disease pathology and therapeutic targets. Integrating HOI with genomic, proteomic, and metabolomic data may improve its utility in personalized medicine, enabling more precise and effective treatment strategies.[44]

In conclusion, this study successfully optimized a chemically induced hypoxia assay using the OcclusionChip platform, establishing the HOI as a reliable and clinically relevant measure of RBC deformability in SCD. The assay's correlation with key clinical biomarkers and its ability to evaluate therapeutic efficacy make it valuable for advancing SCD research and improving patient care. Continued refinement and validation of this assay could enhance the precision and personalization of SCD management strategies, ultimately leading to better clinical outcomes for individuals affected by this debilitating disease.

Author contributions

ZS and UAG conceptualized the idea. ZS, YD, and SO assisted with the planning and execution of clinical sample acquisition and testing, including human subject research protocol development, subject recruitment, and blood sample collection. ZS, YD, PF, CA, MS, YBL, PM, and UAG performed experiments, investigation, data analysis, and visualization. UAG and supervised the work. UAG acquired funding and administrated the project. ZS drafted the original manuscript, and all authors reviewed and edited the manuscript.

Conflicts of interest

UAG and Case Western Reserve University have financial interests in Hemex Health Inc. UAG and Case Western Reserve University have financial interests in BioChip Labs Inc. UAG and Case Western Reserve University have financial interests in Xatek Inc. UAG has financial interests in DxNow Inc. Financial interests include licensed intellectual property, stock ownership, research funding, employment, and consulting. Hemex Health Inc. offers point-of-care diagnostics for hemoglobin disorders, anemia, and malaria. BioChip Labs Inc. offers commercial clinical microfluidic biomarker assays for inherited or acquired blood disorders. Xatek Inc. offers point-of-care global assays to evaluate the hemostatic process. DxNow Inc. offers microfluidic and bio-imaging technologies for *in vitro* fertilization, forensics, and diagnostics. The competing interests of Case Western Reserve University employees are overseen and managed by the Conflict of Interests Committee according to a Conflict-of-Interest Management Plan.

Data availability

Supplementary information is available. See DOI: **https://doi.org/10.1039/D5LC00264H**.

The corresponding author of this publication will fulfill all reasonable requests for materials and data.

Acknowledgements

The authors acknowledge the following funding sources: National Heart Lung and Blood Institute Small Business Innovation Research Program grants: R41HL172662, and R44HL140739; National Institute of Diabetes and Digestive and Kidney Diseases Small Business Innovation Research Program grant R42DK119048; NIH Fogarty International Center D43TW012260, and Case-Coulter Translational Research Partnership pilot award. Zoe Sekyonda acknowledges the American Society of Hematology (ASH) Graduate Hematology Award. This article's contents are solely the authors' responsibility and do not necessarily represent the official views of the National Institutes of Health.

References

1 G. J. Kato, F. B. Piel, C. D. Reid, M. H. Gaston, K. Ohene-Frempong, L. Krishnamurti, W. R. Smith, J. A. Panepinto, D. J. Weatherall, F. F. Costa and E. P. Vichinsky, *Nat. Rev. Dis. Primers*, 2018, **4**, 18010.
2 C. D'Costa, O. Sharma, R. Manna, M. Singh, S. Singh, S. Singh, A. Mahto, P. Govil, S. Satti, N. Mehendale, Y. Italia and D. Paul, *Bioeng. Transl. Med.*, 2024, **9**, e10643.
3 D. C. Rees, T. N. Williams and M. T. Gladwin, *Lancet*, 2010, **376**, 2018–2031.
4 C. C. da Guarda, S. Yahouédéhou, R. P. Santiago, J. Neres, C. F. L. Fernandes, M. M. Aleluia, C. V. B. Figueiredo, L. M. Fiuza, S. P. Carvalho, R. M. Oliveira, C. A. Fonseca, U. S. Ndidi, V. M. L. Nascimento, L. C. Rocha and M. S. Goncalves, *PLoS One*, 2020, **15**, e0228399.
5 P. Sundd, M. T. Gladwin and E. M. Novelli, *Annu. Rev. Pathol.*, 2019, **14**, 263–292.
6 C. Lavazec, G. Deplaine, I. Safeukui, S. Perrot, G. Milon, O. Mercereau-Puijalon, P. H. David and P. Buffet, *Methods Mol. Biol.*, 2013, **923**, 291–297.
7 R. M. Johnson, *Methods Enzymol.*, 1989, **173**, 35–54.
8 M. Musielak, *Clin. Hemorheol. Microcirc.*, 2009, **42**, 47–64.
9 Y. Man, R. An, K. Monchamp, Z. Sekyonda, E. Kucukal, C. Federici, W. J. Wulftange, U. Goreke, A. Bode, V. A. Sheehan and U. A. Gurkan, *Front. Physiol.*, 2022, **13**, 954106.
10 N. Z. Piety, J. Stutz, N. Yilmaz, H. Xia, T. Yoshida and S. S. Shevkoplyas, *Sci. Rep.*, 2021, **11**, 604.
11 A. Nardo-Marino, J. Petersen, J. N. Brewin, H. Birgens, T. N. Williams, J. A. L. Kurtzhals, D. C. Rees and A. Glenthøj, *Br. J. Haematol.*, 2022, **197**, 609–617.
12 Y. Man, E. Kucukal, R. An, Q. D. Watson, J. Bosch, P. A. Zimmerman, J. A. Little and U. A. Gurkan, *Lab Chip*, 2020, **20**, 2086–2099.

13 Y. Man, E. Kucukal, R. An, A. Bode, J. A. Little and U. A. Gurkan, *Microcirculation*, 2021, **28**, e12662.
14 M. Kim, Y. Alapan, A. Adhikari, J. A. Little and U. A. Gurkan, *Microcirculation*, 2017, **24**, e12374.
15 Y. Man, Z. Sekyonda, K. Monchamp, R. An, E. Kucukal, C. Federici, L. V. Nayak, J. A. Little and U. A. Gurkan, *Blood*, 2021, **138**, 966.
16 W. A. Eaton and H. F. Bunn, *Blood*, 2017, **129**, 2719–2726.
17 E. Mahase, *BMJ*, 2024, **387**, q2147.
18 M. S. Kim and V. Prasad, *Am. J. Hematol.*, 2025, **100**, 922–924.
19 K. Dufu, C. Alt, S. Strutt, J. Partridge, T. Tang, V. Siu, H. Liao-Zou, P. Rademacher, A. T. Williams, C. R. Muller, X. Geng, M. P. Pochron, A. N. Dang, P. Cabrales, Z. Li, D. Oksenberg and B. E. Cathers, *Br. J. Haematol.*, 2023, **202**, 173–183.
20 P. Schroeder, K. Fulzele, S. Forsyth, M. D. Ribadeneira, S. Guichard, E. Wilker, C. G. Marshall, A. Drake, R. Fessler, D. G. Konstantinidis, K. G. Seu and T. A. Kalfa, *J. Pharmacol. Exp. Ther.*, 2022, **380**, 210–219.
21 A. Shrestha, M. Chi, K. Wagner, A. Malik, J. Korpik, A. Drake, K. Fulzele, S. Guichard and P. Malik, *Blood Adv.*, 2021, **5**, 2385–2390.
22 A. Hannemann, D. C. Rees, J. N. Brewin, A. Noe, B. Low and J. S. Gibson, *Br. J. Haematol.*, 2018, **182**, 567–578.
23 P. Klaihmon, S. Vimonpatranon, E. Noulsri, S. Lertthammakiat, U. Anurathapan, N. Sirachainan, S. Hongeng and K. Pattanapanyasat, *Ann. Hematol.*, 2017, **96**, 1741–1747.
24 T. Banerjee and F. A. Kuypers, *Br. J. Haematol.*, 2004, **124**, 391–402.
25 J. G. Mohanty, E. Nagababu and J. M. Rifkind, *Front. Physiol.*, 2014, **5**, 84.
26 T. Jang, M. Poplawska, E. Cimpeanu, G. Mo, D. Dutta and S. H. Lim, *J. Transl. Med.*, 2021, **19**, 397.
27 M. P. Wautier, E. Héron, J. Picot, Y. Colin, O. Hermine and J. L. Wautier, *J. Thromb. Haemostasis*, 2011, **9**, 1049–1055.
28 N. W. Wairimu, P. Wairagu, K. W. Chepukosi, G. F. Obiero, P. W. Okanya, A. O. Isaac and J. N. Nyariki, *J. Toxicol.*, 2023, **2023**, 7058016.
29 T. M. Mikobi, P. Lukusa Tshilobo, M. N. Aloni, G. Mvumbi Lelo, P. Z. Akilimali, J. J. Muyembe-Tamfum, V. Race, G. Matthijs and J. M. Mbuyi Mwamba, *PLoS One*, 2015, **10**, e0123568.
30 G. J. Kato, V. McGowan, R. F. Machado, J. A. Little, J. t. Taylor, C. R. Morris, J. S. Nichols, X. Wang, M. Poljakovic, S. M. Morris Jr. and M. T. Gladwin, *Blood*, 2006, **107**, 2279–2285.
31 O. T. Gbotosho, J. Gollamudi and H. I. Hyacinth, *Biomolecules*, 2023, **13**(2), 381.
32 S. Charache, M. L. Terrin, R. D. Moore, G. J. Dover, F. B. Barton, S. V. Eckert, R. P. McMahon and D. R. Bonds, *N. Engl. J. Med.*, 1995, **332**, 1317–1322.
33 K. Matthews, E. S. Lamoureux, M.-E. Myrand-Lapierre, S. P. Duffy and H. Ma, *Lab Chip*, 2022, **22**, 1254–1274.
34 R. Skalak and P. I. Branemark, *Science*, 1969, **164**, 717–719.
35 M. A. E. Rab, C. K. Kanne, C. Boisson, J. Bos, B. A. van Oirschot, M. E. Houwing, C. Renoux, M. Bartels, A. W. Rijneveld, E. Nur, M. H. Cnossen, P. Joly, E. Nader, R. Fort, P. Connes, R. van Wijk, V. A. Sheehan and E. J. van Beers, *Blood Adv.*, 2024, **8**, 276–286.
36 E. Vichinsky, C. C. Hoppe, K. I. Ataga, R. E. Ware, V. Nduba, A. El-Beshlawy, H. Hassab, M. M. Achebe, S. Alkindi, R. C. Brown, D. L. Diuguid, P. Telfer, D. A. Tsitsikas, A. Elghandour, V. R. Gordeuk, J. Kanter, M. R. Abboud, J. Lehrer-Graiwer, M. Tonda, A. Intondi, B. Tong and J. Howard, *N. Engl. J. Med.*, 2019, **381**, 509–519.
37 J. S. Gibson and D. C. Rees, *Expert Opin. Ther. Targets*, 2023, **27**, 133–149.
38 M. J. van Dijk, J. R. de Wilde, M. Bartels, K. H. Kuo, A. Glenthøj, M. A. Rab, E. J. van Beers and R. van Wijk, *Blood Rev.*, 2023, 101103.
39 C. C. John, R. O. Opoka, T. S. Latham, H. A. Hume, C. Nabaggala, P. Kasirye, C. M. Ndugwa, A. Lane and R. E. Ware, *N. Engl. J. Med.*, 2020, **382**, 2524–2533.
40 C. C. John, R. Opoka, T. Latham, H. Hume, M. Nakafeero, P. Kasirye, C. Ndugwa, A. Lane and R. E. Ware, *Blood*, 2019, **134**, 520.
41 E. Du, M. Diez-Silva, G. J. Kato, M. Dao and S. Suresh, *Proc. Natl. Acad. Sci. U. S. A.*, 2015, **112**(5), 1422–1427.
42 R. E. Horton, *Microcirculation*, 2017, **24**, e12373.
43 A. Aich, Y. Lamarre, D. P. Sacomani, S. Kashima, D. T. Covas and L. G. de la Torre, *Front. Mol. Biosci.*, 2020, **7**, 558982.
44 M. Jacob, A. L. Lopata, M. Dasouki and A. M. Abdel Rahman, *Mass Spectrom. Rev.*, 2019, **38**, 221–238.